Free Radical Biology and Medicine 148 (2020) 60–69

Contents lists available at ScienceDirect

Free Radical Biology and Medicine

journal homepage: www.elsevier.com/locate/freeradbiomed

Original article

Isoform-selective NADPH oxidase inhibitor panel for pharmacological target validation

Vu Thao-Vi Dao[a,b,1], Mahmoud H. Elbatreek[a,c,1], Sebastian Altenhöfer[a], Ana I. Casas[a], Mayra P. Pachado[a], Christopher T. Neullens[a], Ulla G. Knaus[d], Harald H.H.W. Schmidt[a,*]

[a] Department for Pharmacology and Personalised Medicine, FHML, Maastricht University, Maastricht, the Netherlands
[b] Department of Psychiatry, Psychosomatic Medicine and Psychotherapy, University Hospital Frankfurt, Frankfurt, Germany
[c] Department for Pharmacology and Toxicology, Faculty of Pharmacy, Zagazig University, Zagazig, Egypt
[d] Conway Institute, University College Dublin, Belfield, Dublin, Ireland

ARTICLE INFO

Keywords:
NADPH oxidase
NOX inhibitors
Reactive oxygen species
Target validation

ABSTRACT

Dysfunctional reactive oxygen species (ROS) signaling is considered an important disease mechanism. Therapeutically, non-selective scavenging of ROS by antioxidants, however, has failed in multiple clinical trials to provide patient benefit. Instead, pharmacological modulation of disease-relevant, enzymatic sources of ROS appears to be an alternative, more promising and meanwhile successfully validated approach. With respect to targets, the family of NADPH oxidases (NOX) stands out as main and dedicated ROS sources. Validation of the different NOX isoforms has been mainly through genetically modified rodent models and is lagging behind in other species. It is unclear whether the different NOX isoforms are sufficiently distinct to allow selective pharmacological modulation. Here we show for five widely used NOX inhibitors that isoform selectivity can be achieved, although individual compound specificity is as yet insufficient. NOX1 was most potently (IC_{50}) targeted by ML171 (0.1 μM); NOX2, by VAS2870 (0.7 μM); NOX4, by M13 (0.01 μM) and NOX5, by ML090 (0.01 μM). In addition, some non-specific antioxidant and assay artefacts may limit the interpretation of data, which included, surprisingly, the clinically advanced NOX inhibitor, GKT136901. In a human ischemic blood-brain barrier hyperpermeability model where genetic target validation is not an option, we provide proof-of-principle that pharmacological target validation for different NOX isoforms is possible by applying an inhibitor panel at IC_{50} concentrations. Moreover, our findings encourage further lead optimization and development efforts for isoform-selective NOX inhibitors in different indications.

1. Introduction

Reactive oxygen species (ROS) signaling may become dysfunctional through (i) ROS formation in unphysiological high amounts, and/or (ii) at (sub)cellular locations, where normally no or only very low amounts of ROS are formed, and/or (iii) switch in the predominant ROS type, e.g. superoxide instead of hydrogen peroxide. Any of these mechanisms may lead to disease. The initial approach to translate of this hypothesis into therapeutic application by the use of antioxidants that scavenge ROS has consistently failed [1], in some cases even increasing mortality [2–4]. This paradox was initially explained by these compounds may have been underdosed [5], thereby not reaching efficacy. It is now understood, however, that ROS are not only harmful metabolic by-products, but also serve important protective, metabolic and signaling functions, such as the regulation of cell proliferation, differentiation, migration and survival, innate immune response, vascular tone, neuronal signaling as well as inflammation [6–9]. Antioxidants obviously interfere with both qualities of ROS, the physiological and pathophysiological ones with overall neutral or even deleterious outcomes. Thus, ROS should not be modulated in a systemic, non-selective manner, but rather by identifying for each disease condition the relevant enzymatic source of ROS and inhibit this by selective pharmacological compounds without touching parallel physiological ROS-dependent processes [10].

ROS can be produced by several sources, dedicated ones and optional ones. These include mitochondrial ROS formation, xanthine oxidase, uncoupled nitric oxide synthase (uc-NOS) and NADPH

* Corresponding author. Department for Pharmacology and Personalised Medicine, FHML, Maastricht University, PO Box 616, 6200 MD, Maastricht, the Netherlands.
E-mail address: hschmidt@ppmlab.net (H.H.H.W. Schmidt).
[1] Both authors contributed equally.

https://doi.org/10.1016/j.freeradbiomed.2019.12.038
Received 19 December 2019; Accepted 24 December 2019
Available online 25 December 2019
0891-5849/ © 2020 The Authors. Published by Elsevier Inc. This is an open access article under the CC BY license (http://creativecommons.org/licenses/BY/4.0/).

oxidases (NOX) [11,12]. Of these, only NOX enzymes produce ROS as their sole and primary function; all others, only as a byproduct or upon damage. With respect to the different NOX isoforms, disease relevance has been suggested for NOX1 in diabetic atherosclerosis [13] and retinopathy [14]; NOX2, in neurodegeneration [15]; NOX4, in stroke [16], diabetic nephropathy [17] and neuropathic pain [18]; and NOX5, stroke [19], diabetic nephropathy [20,21], hypertension [22] and coronary artery disease [23]. Target validation in these cases, however, has been done primarily by gene knock-out (as reviewed in Ref. [24]) due to the lack of selective NOX inhibitors and, in the case of NOX5 [20], by knock-in technology. This approach has limiting target validation to mice and, in the case of NOX4, also to rat [16].

Source-specific pharmacological inhibition is important though. Similar to antioxidants, non-selective inhibition of NOX isoforms, i.e. inhibiting two or more NOX isoforms might be as ineffective or deleterious as antioxidants. For example, in diabetes-accelerated atherosclerosis, inhibition of NOX1 is protective [25], inhibition of NOX4 is detrimental [26,27] and inhibition of NOX2 is associated with increased mortality [25]. Therefore, for target validation in other species than mice and rats and clinical translation, isoform-selective NOX inhibitors are desirable. It is unclear, however, whether this is or will be achievable given the fact that all five NOX isoforms (NOX1, NOX2, NOX3, NOX4 and NOX5) are similarly structured transmembrane proteins containing highly conserved catalytic heme, FAD and NADPH binding sites. Some degree of variability derives from more (NOX1 and NOX2) or less (NOX4 and NOX5) binding partners or a unique regulation by calcium (NOX5) [28]. Furthermore, for each compound two potential sources of assay error or artifact need to be considered: (i) direct scavenging of ROS [29,30] instead of or in addition to NOX inhibition; and (ii) interference with the ROS detection probes [31,32]. We therefore here examine some of the best characterized and widely used NOX inhibitors, VAS2870, ML171, GKT136901, M13 and ML090 in a 'whole-cell' assay approach by analyzing isoform selectivity, possible assay interference and direct ROS-scavenging capacity.

2. Material and methods

2.1. Chemicals and reagents

Dulbecco's Modified Eagle Medium (DMEM) with GlutaMax, Roswell Park Memorial Institute (RPMI)-1640 medium with L-glutamine, Hanks' Buffered Salt Solution (HBSS) [Ingredients (mg/L); calcium chloride anhydrous (140), magnesium chloride hexahydrate (100), magnesium sulphate heptahydrate (100), potassium chloride (400), potassium phosphate monobasic (60), sodium bicarbonate (350), sodium chloride (8000), sodium phosphate dibasic anhydrous (48) and D-glucose (1000)] and phosphate buffered saline (PBS), pH 7.4 [Ingredients (mg/L); potassium phosphate monobasic (144), sodium chloride (9000), and sodium phosphate dibasic (795)] were purchased from GIBCO/Life Technologies. Krebs-Ringer Phosphate Glucose (KRPG) buffer, PH 7.35 [Ingredients (mg/L); sodium chloride (847.38), sodium dihydrogen phosphate dihydrate (88.9), potassium chloride (36.23), calcium chloride dihydrate (7.939), magnesium sulphate heptahydrate (30) and D-glucose (109)] was prepared in house. Fetal bovine serum (FBS), fetal calf serum (FCS), 2-acetylphenothiazine (ML171), 5,12-dihydroquinoxalino(2,3-B)quinoxaline (ML090), phorbol 12-myristate 13-acetate (PMA), calcein, diphenyleneiodonium chloride (DPI), dextran sulphate, dimethyl sulfoxide (DMSO), Luminol, sodium salt, superoxide dismutase (SOD), Geneticin antibiotic (G418), ionomycin calcium salt ready to made solution and penicillin/streptomycin solution were purchased from Sigma–Aldrich. 3-benzyl-7-(2-benzoxazolyl) thio-1,2,3-triazolo [4,5-di] pyrimidine (VAS2870) was provided by Vasopharm; the pyrazolopyridine derivative GKT 136901, by GenKyoTex; M13, by Glucox Biotech. Amplex Red and horseradish peroxidase (HRP) were purchased from Invitrogen, CA, USA. The FuGENE® 6 transfection reagent was purchased from Promega. Endothelial growth medium (EGM-2 MV) [Ingredients (ml/500 ml medium); 500 ml of Endothelial Basal Medium-2 (EBMTM-2 Medium) and the following growth supplements: human Epidermal Growth Factor (hEGF), 0.5; Vascular Endothelial Growth Factor (VEGF), 0.5; R3-Insulin-like Growth Factor-1 (R3-IGF-1), 0.5 ml; Ascorbic Acid, 0.5; Hydrocortisone, 0.2; human Fibroblast Growth Factor-Beta (hFGF-β), 2.0; FBS, 25.0; Gentamicin/Amphotericin-B (GA), 0.5] was purchased from Lonza Bioscience.

2.2. Cell culture and transfections

Human embryonic kidney 293 (HEK293) cells cultured in DMEM medium containing 5% FBS were transfected with three plasmids [human NADPH oxidase organizer 1 (NOXO1), NADPH oxidase activator 1 (NOXA1) and NADPH oxidase 1 (NOX1)] to express active NOX1. However, to express active NOX4 or NOX5 in HEK293, it is sufficient to transfect the cells with only one plasmid, i.e. NOX4 or NOX5, respectively. All plasmids were confirmed by sequencing. Briefly, HEK293 cells were transfected with pcDNA control plasmid (vector control), NOX4 or NOX5 or triple transfected with NOX1, NOXO1 and NOXA1 using FuGENE6 transfection reagent (Promega) followed by ROS measurement after 48h. In all experiments, the NOX inhibitors were tested in the same preparation of transfected cells to ensure comparibility. To measure NOX2 activity, as described previously [32], superoxide was measured in human promyelocytic leukemia (HL-60) cells (ATCC-No. CCL 240) that were cultured in RPMI-1640 medium with 5% FCS, penicillin (100 $U \cdot mL^{-1}$), streptomycin (100 $\mu g \cdot mL^{-1}$) and glutamine (2 mM). Cell suspensions (26×10^6 $cells \cdot mL^{-1}$) were incubated with 1.25% DMSO per 75 cm^2 tissue culture flask (TCF-75) for 7 days to induce differentiation into granulocyte-like cells that were then centrifuged at 300xG, washed with HBSS and re-suspended in HBSS to the final seeding density needed for the experiment (5×10^5 cells/well in 96 well plate).

2.3. RNA extraction and cDNA synthesis

Briefly, HEK293 cells were trypsinized and collected in centrifuge tubes. Both HEK293 and HL-60 cells were then centrifuged for 5 min at 300xg and supernatants removed. Pelleted cells were lyzed by adding lysis buffer (provided with the kit) and then homogenized by passing the lysate 5 times through a blunt 20-gauge needle (0.9 mm diameter) fitted to an RNase-free syringe. RNA was extracted using RNeasy® Micro Kit (Qiagen) according to the manufacturer's kit manual.

cDNA was synthesized from 1 μg total RNA in 20 μl reactions using High Capacity cDNA Reverse Transcription Kit (Thermo Fisher Scientific). Briefly, reverse transcription master mix containing, reverse transcription buffer, deoxyribonucleotide triphosphate (dNTP) mix, reverse transcription random primers, Multiscribe™ reverse transcriptase, RNase inhibitor and nuclease-free water, was prepared. Then, 10 μl of the master mix and 10 μl RNA were pipetted in each well of 96-well plate. The plate was then sealed and centrifuged to spin down the contents and to eliminate any air bubbles. Afterwards, the plate was loaded into the thermal cycler. The PCR conditions were as follows: 10 min at 25 °C, followed by 120 min at 37 °C, followed by 5 min at 85 °C. After synthesis, the cDNA was stored at −20 °C.

2.4. Quantitative Real-Time PCR

RT-qPCR was performed on CFX96™ Real-Time PCR Detection System (Bio-Rad). All reactions were performed in triplicates in a total volume of 20 μl each using TaqMan® Universal PCR Master Mix (Applied Biosystems- Life Technologies) according to manufacturer's instructions. 3 μl cDNA was used as template and pre-designed TaqMan® primers of β-actin, Nox1, Nox2, Nox4 and Nox5 were used. The specific assay ID for the primers used are shown in Supplementary Table S1. The standard PCR conditions were as follows: 10 min at 95 °C,

followed by 15 s at 95 °C and 1 min at 60 °C, 59 repeats. The amount of mRNA was normalized to the measured expression of β-actin mRNA.

2.5. ROS measurement in intact cells

2.5.1. Luminol assay

To measure NOX1 activity, superoxide from vector-transfected or NOX1-transfected HEK293 cells was measured by luminol-enhanced chemiluminescence in white plates as follows. HEK293 cells were cultured in DMEM medium containing 5% FBS and then transfected with NOX1, NOXO1 and NOXA1 plasmids using FuGENE®6 transfection reagent. After 48 h, cells were detached by adding trypsin and then re-suspended in KRPG buffer. Each 50 μl of cell suspension consisted of 100,000 cells was added to each well (in triplicate) in a 96-well plate and incubated at 37 °C for 60 min. After 1 h of incubation, 50 μl reaction buffer (containing 6.4 U/ml HRP and 0.4 mM luminol in KRPG buffer) was added to the 50 μl cell suspension so that the total volume of assay was 100 μl. Cells were then stimulated by addition of 0.5 μM phorbol 12-myristate 13-acetate (PMA; PKC activator). Superoxide generation was detected by monitoring relative light units (RLU) with a Wallac luminometer Victor2 at 37 °C for 60 min. Superoxide dismutase (SOD) was added as control before PMA stimulation in selected wells.

2.5.2. Amplex Red assay

To measure the activity of NOX4 and NOX5, H_2O_2 production was measured in HEK293 cells by measuring Amplex Red fluorescence using Amplex™ Red Hydrogen Peroxide/Peroxidase Assay Kit (ThermoFiher Scientific). For the measurement, vector-transfected HEK293 cells or HEK293 cells transfected with NOX4 or NOX5 were trypsinized, counted, washed and re-suspended in KRPG buffer. NOX inhibitors dissolved in DMSO or solvent control (0.5% DMSO) were added to respective wells of a black 96-well plate and 50 μl of a reaction mixture containing 0.1 $U{\cdot}mL^{-1}$ HRP and 50 μM Amplex Red reagent was added to each well according to the kit manual and incubated at 37 °C for 10 min. Thereafter, 100,000 of respective HEK293 cells or solvent control in 50 μl of KPRG buffer were added to each well. Amplex Red fluorescence was measured immediately at excitation (530–560 nm) and emission (~590 nm) at 37 °C for 60 min. HEK293 cells expressing NOX5 were activated by the Ca^{2+} ionophore ionomycin (40 μM).

2.5.3. Cytochrome C assay

To measure NOX2 activity, superoxide production in HL-60 cells was measured by cytochrome C reduction as described previously [32]. Briefly, HL-60 cells were cultured in RPMI-1640 medium with 5% FCS, penicillin (100 $U{\bullet}mL^{-1}$), streptomycin (100 $\mu g{\bullet}mL^{-1}$) and glutamine (2 mM). Cell suspensions (26×10^6 $cells{\bullet}mL^{-1}$) were incubated with 1.25% DMSO per TCF-75 for 7 days to induce differentiation into granulocyte-like cells that were then centrifuged at 300xG, washed with HBSS and re-suspended in HBSS to the final seeding density needed for the experiment (5×10^5 cells/well in 96 well plate). Cytochrome C (100 μM) and the inhibitors were added to the DMSO-differentiated HL-60 cell suspension then a basal reading was performed at 540 nm (isosbestic point of cytochrome C) and 550 nm (SpectraMax 340; Molecular Devices, Sunnyvale, CA, USA). Subsequently, the oxidative burst was initiated by the addition of 100 nM PMA. After incubation for 60 min at 37 °C the absorbance was measured. Signals were normalized to the basal readings. In addition, SOD was added as control before PMA stimulation in selected wells.

2.6. Superoxide measurement in cell-free assays

Xanthine (X; final concentration: 50 μm) and cytochrome C (final concentration: 100 μm) were dissolved in HBSS, and 100 μL aliquots of this solution were transferred to individual wells of a 96-well plate. After addition of the oxidase inhibitors, the mixtures were allowed to equilibrate for 20 min. The reaction was started by the addition of 100 μL xanthine oxidase (XO) (final concentration: 5 $mU{\cdot}mL^{-1}$), and absorbance at 540 and 550 nm was recorded 10 min after the start of the reaction. Superoxide production was calculated by normalization to the signals obtained at 540 nm. Similar experiments were performed with 0.4 mM luminol instead of cytochrome C. After 20 min equilibration, the reaction was started with XO (1 $mU{\cdot}mL^{-1}$), and chemiluminescence was subsequently recorded for 20 min in a Fluoroscan FL microplate reader. Signals were calculated as area under curve (AUC) and normalized to the X/XO-derived control signal. Accordingly, a counter screen has been performed with cytochrome C or luminol without X/XO-generated superoxide.

2.7. H_2O_2 measurement in cell-free system

The fluorescence of Amplex Red was measured in the presence and absence of H_2O_2 (0.25 μM), reflecting NOX4 and NOX5 output. After addition of inhibitors and 50 μl Amplex Red reaction mixture containing 100 $U{\cdot}mL^{-1}$ HRP and 10 mM Amplex Red to each well, the plate was incubated at 37 °C for 10 min. Thereafter, the plate was read at excitation (530–560 nm) and emission (~590 nm) at 37 °C and for 60 min. Data was calculated as the AUC over 60 min and data were normalized to H_2O_2 output in the absence of inhibitor.

2.8. Cell permeability in HBMECs

For the passive dye diffusion assay, 2×10^4 human brain microvascular endothelial cells (HBMECs) were grown to confluence on membranes of transwell inserts (collagen-coated transwell pore polyester membrane insert; pore size = 3.0 μm (Corning, The Netherlands) Fig. 5A). After 6hrs of ischemia, cells were treated with 0.1 μM ML171, 0.6 μM VAS2870, 1 μM GKT136901, 0.2 μM M13 or 0.01 μM ML090 during 24hrs of re-oxygenation. Thereafter, cell permeability was assessed using Evans Blue (Sigma-Aldrich) (Fig. 5B). First, the medium was removed and previously warmed (37 °C) PBS (1.5 ml) was added to the abluminal side of the insert. Permeability buffer (0.5 ml) containing 4% bovine serum albumin (Sigma-Aldrich) and 0.67 mg/ml Evans blue dye in PBS was loaded on the luminal side of the insert followed by 15 min incubation at 37 °C. The concentration of Evans Blue in the abluminal chamber was measured by determining the absorbance of 200 μl buffer at 630 nm using a microplate reader.

2.9. Statistical analysis

Data analysis was performed using Prism 6.0g software package (GraphPad Software, San Diego, USA). IC_{50} values were calculated with a non-linear regression analysis using an algorithm for sigmoidal dose–response with variable slopes. Results are expressed as means ± SEM. Statistical differences between means were analyzed by one-way ANOVA followed by Bonferroni correction for multiple comparisons. A value of $P < 0.05$ was considered statistically significant.

3. Results

3.1. Gene expression of NOX isoforms

To check the expression of the different NOX isoforms, we analyzed NOX1, 2, 4 and 5 mRNA expression in control vector-transfected HEK293 cells, HEK293 cells transfected with NOX1, 2, 4 and 5 and HL-60 cells. NOX isoforms mRNA expression was measured by RT-qPCR and mRNA levels were normalized to the expression of β-actin.

As reported previously [28,33], NOX1 was expressed in NOX1-transfected HEK293 cells (Fig. 1A), NOX2 in HL-60 (Fig. 1B), NOX4 in NOX4-transfected HEK293 (Fig. 1C) and NOX5 in NOX5-transfected HEK293 (Fig. 1D) and were below detection limit (defined as 100 times lower than in the respective NOX overexpressing cells) in all other cell preparations. Notably, the expression of NOX isoforms did not change after treatment with the respective assay conditions i.e. luminol for NOX1, cytochrome C for NOX2 and Amplex Red for NOX4 and NOX5 (Fig. 1A–1D).

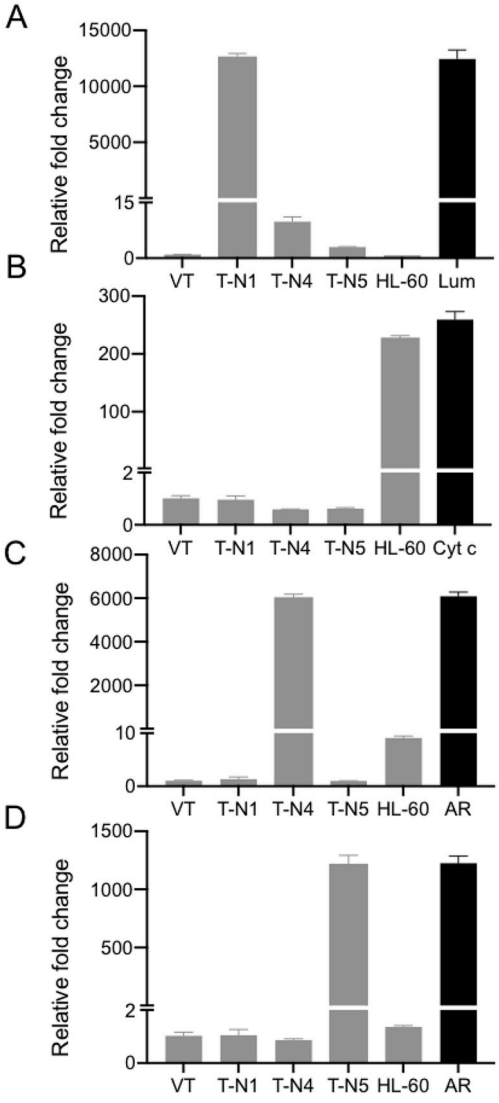

Fig. 1. RT-qPCR of NOX isoforms mRNA expression in HEK293 and HL-60 cells. NOX isoforms mRNA levels were measured and normalized to the expression of β-actin. Vector-transfected HEK293 cells (VT) were used as control. To check whether assay reagents interfere with NOXs gene expression, HEK293 cells transfected with NOX1 (T-N1) were treated with luminol (Lum), HL-60 cells were treated with cytochrome C (Cyt *c*) and HEK293 cells transfected with NOX4 (T-N4) or NOX5 (T-N5) were treated with Amplex Red (AR). A) mRNA levels of NOX1. B) mRNA levels of NOX2. C) mRNA levels of NOX4. D) mRNA levels of NOX5. Data are presented as the mean ± SEM of three experiments.

3.2. NOX pharmacological isoform selectivity

To characterize the NOX isoform selectivity of the current second-generation NOX inhibitors we determined concentration-dependency and efficacy of GKT136901, ML171, VAS2870, M13 and ML090 on NOX1, 2, 4, and 5 (Fig. 2A). Our preference was for cell (lines) expressing a specific NOX isoform in a highly selective manner and ideally physiologically. The latter is only known for NOX2 and HL-60 cells [34,35]. For NOX1, NOX4 and NOX5, there is, to our knowledge, no such native human cell line. Therefore, for these three isoforms we used transiently transfected HEK-293 cells, using previously validated methodology [29]. One major limitation of this approach is that validation of the compounds on two different preparations i.e. transfected vs. constitutive expressing cells can affect the dose-response correlations and make it hard to extrapolate data to the real physiological scenarios.

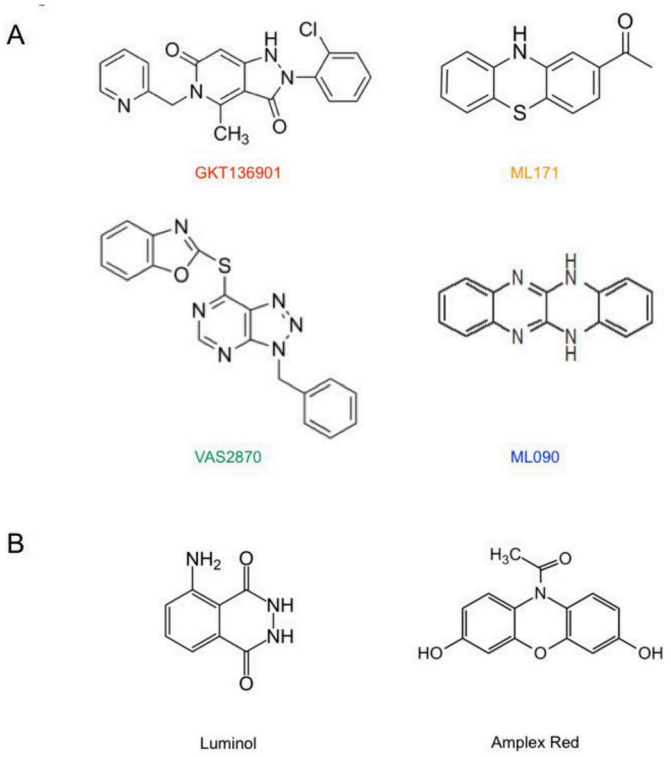

Fig. 2. Chemical structures. Chemical structure of (A) NOX inhibitors (red, orange, green and blue text) and (B) ROS detection probes (black text) used in the study. (For interpretation of the references to colour in this figure legend, the reader is referred to the Web version of this article).

NOX2 expressing HL-60 cells or HEK293 cells transfected with NOX1, NOX4 or NOX5 were incubated in presence of increasing concentrations of each compound. ROS generation was subsequently induced by PMA to stimulate NOX1, NOX2 and NOX5, which was assayed in the presence of ionomycin. Thereafter, ROS production was assayed using a panel of cellular assays with structurally unrelated probes; *i.e.* Amplex Red, luminol or cytochrome C (Fig. 2B). Amplex Red was used to quantify extracellular H_2O_2 [36], while luminol-based chemiluminescence and cytochrome C-reduction were used to quantify superoxide generation. These probes were chosen based on previous data. Luminol assay has been validated to measure low superoxide-producing NOX1 activity [37,38], while cytochrome C is used for high superoxide-output NOX2 activity [34,39] and Amplex Red for testing hydrogen peroxide formation from NOX4 [40–42] and NOX5 [43,44] activities. As controls, medium, vector-transfected HEK293 cells and non-stimulated HL-60 cells were used (Fig. S1), in addition, PMA or PMA plus ionomycin did not stimulate cell controls i.e. vector-transfected HEK293 cells and non-stimulated HL-60 cells (Fig. S2).

NOX isoform concentration-response curves for GKT136901, ML171, VAS2870, M13 and ML090 were constructed (Fig. 3; see Table 1 for IC_{50} values). GKT136901 (Fig. 3A) showed selectivity for NOX1 over NOX4 and NOX5 inhibition while NOX2 inhibition was not observed. The same holds true for ML171 (Fig. 3B) which is more selective for NOX1 compared to NOX4 and NOX5. VAS2870 (Fig. 3C) displayed NOX2 over NOX1 and NOX4 selective inhibition and also slightly inhibited NOX5. The GlucoxBiotech compound M13 (Fig. 3D) showed almost selective NOX4 inhibition but NOX2 (with low E_{max}) and NOX1 (at high concentrations) inhibition was observed as well. Finally, ML090 (Fig. 3E) inhibited NOX5, NOX1 and NOX4 with comparable IC_{50} values but enhanced E_{max} for NOX5 inhibition. These data suggest that NOX inhibitors indeed display differential isoform targeting, albeit the single compound selectivity is yet not sufficient. Therefore, combined analysis of a NOX inhibitor panel with sufficient differential potencies and selectivities is suggested.

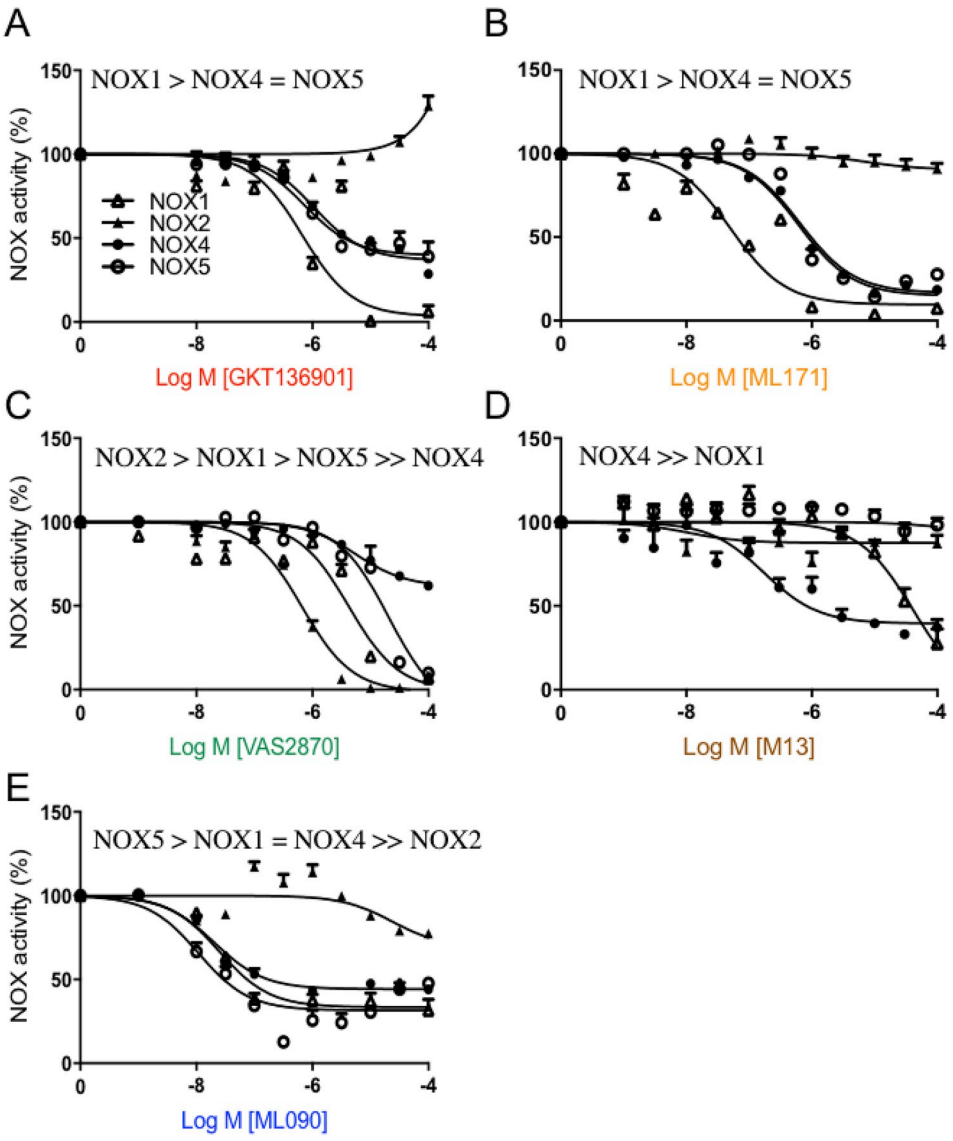

Fig. 3. NOX inhibitors display isoform selectivity. ROS production was assessed in whole cells using assays measuring superoxide production by NOX1 (luminol assay) or NOX2 (cytochrome C assay) and H_2O_2 production by NOX4 or NOX5 (Amplex Red assay). As illustrated in the figure (A–E), GKT136901 (A), ML171 (B), VAS2870 (C), M13 (D) or ML090 (E) inhibited ROS production with NOX isoform selective IC_{50}. Data are presented as the mean ± SEM of n = 3 independent experiments. 100% is the PMA-induced activation (PMA + ionomycin in case of NOX5) without inhibitors.

Table 1
Potency and efficacy of the five tested NOX inhibitors on different NOS isoforms.

NOX inhibitor		NOX1	NOX2	NOX4	NOX5
GKT136901	IC_{50}	-6.2	> -3	-6.0	-6.1
	E_{max}	**99**	N/A	**71**	61
ML171	IC_{50}	**-7.3**	N/A	-6.2	-6.2
	E_{max}	**96**	09	82	75
VAS2870	IC_{50}	-5.4	**-6.2**	N/A	-4.7
	E_{max}	93	**99**	38	90
M13	IC_{50}	-4.4	N/A	**-6.8**	N/A
	E_{max}	73	12.7	**67**	05
ML090	IC_{50}	-7.6	N/A	-7.7	**-8.0**
	E_{max}	68	23	57	**81**

Footnote: IC_{50}, concentration (log M) for half-maximal inhibition; E_{max}, maximal inhibition as % of control by each inhibitor per isoform. IC_{50} is written as not-applicable (N/A) when E_{max} is less than 50%. Predominant isoform in bold.

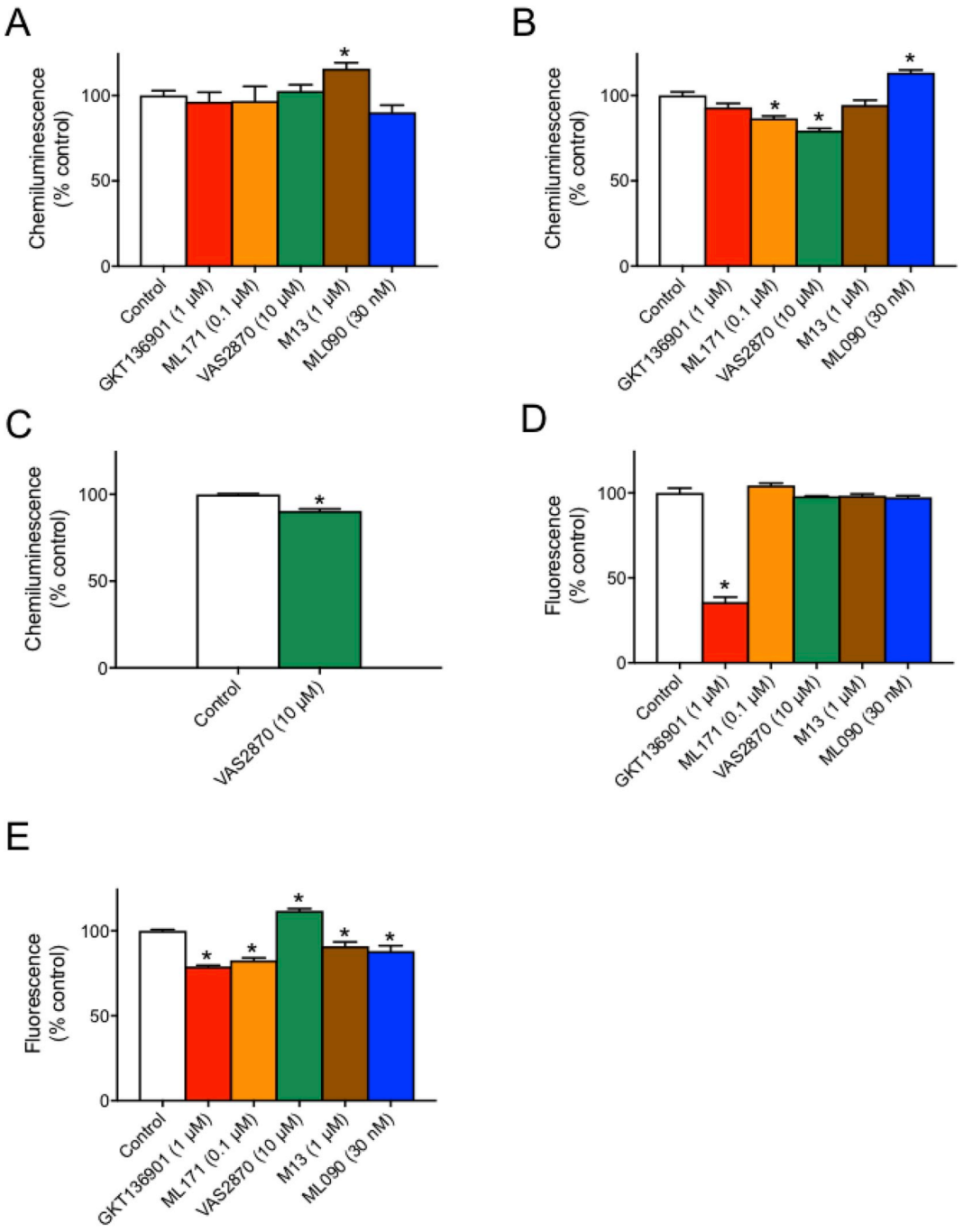

Fig. 4. NOX inhibitors display interference with ROS assays. A/B) To study possible interference of GKT136901, ML171, VAS2870, M13 or ML090 with luminol-based measurements cell-free luminol assays were used. In these assays, ROS production generated by X/XO was enhanced by M13 (A) but not by GKT136901, ML171, VAS2870 or ML090. Moreover, chemiluminescence produced by luminol only was inhibited by ML171 and VAS2870, enhanced by ML090 and not affected by GKT136901 or M13, respectively (B). C) Possible assay interference by NOX2-specific VAS2870 was assessed by studying cytochrome C reduction in presence of X/XO-derived ROS in a cell-free system. Presence of VAS2870 slightly, but significantly reduced chemiluminescence. D/E) The possibility of interference between GKT136901, ML171, VAS2870, M13 or ML090 and Amplex Red-based assays was studied using cell-free Amplex Red assays. In these assays, Fluorescence generated by H_2O_2 was significantly inhibited by GKT136901 (D) but not by ML171, VAS2870, M13 or ML090 (D). Moreover, fluorescence produced by Amplex Red only was inhibited by GKT136901, ML171, M13 and ML090 while it was enhanced by VAS2870 (E). Data are presented as the mean ± SEM of three experiments. *P < 0.05.

3.3. Non-specific antioxidant and assay artefacts

To screen for possible assay interference between GKT136901, ML171, VAS2870, M13 or ML090 and the NOX1 assay, a cell-free system was performed in which each inhibitor was screened in presence of luminol, 1mU/ml xanthine oxidase (XO) and 1 mg xanthine (X) generating superoxide. At concentration 1 μM, GKT136901 did not show interference with either the molecular probe or with the X/XO system (Fig. 4A). Similar findings were obtained with 0.1 μM ML171, 10 μM VAS2870 and 30 nM ML090 (Fig. 4A). In contrast, 1 μM M13 enhanced chemiluminescence (Fig. 4A). To identify direct interactions between assay components and GKT136901, ML171, VAS2870, M13 or ML090 a cell-free counter screen was performed without X/XO-generated ROS. Indeed, ML171 and VAS2870 showed reduction of the luminol-based signal suggesting direct interference with luminol-based chemiluminescence (Fig. 4B). In contrast, in presence of ML090 the

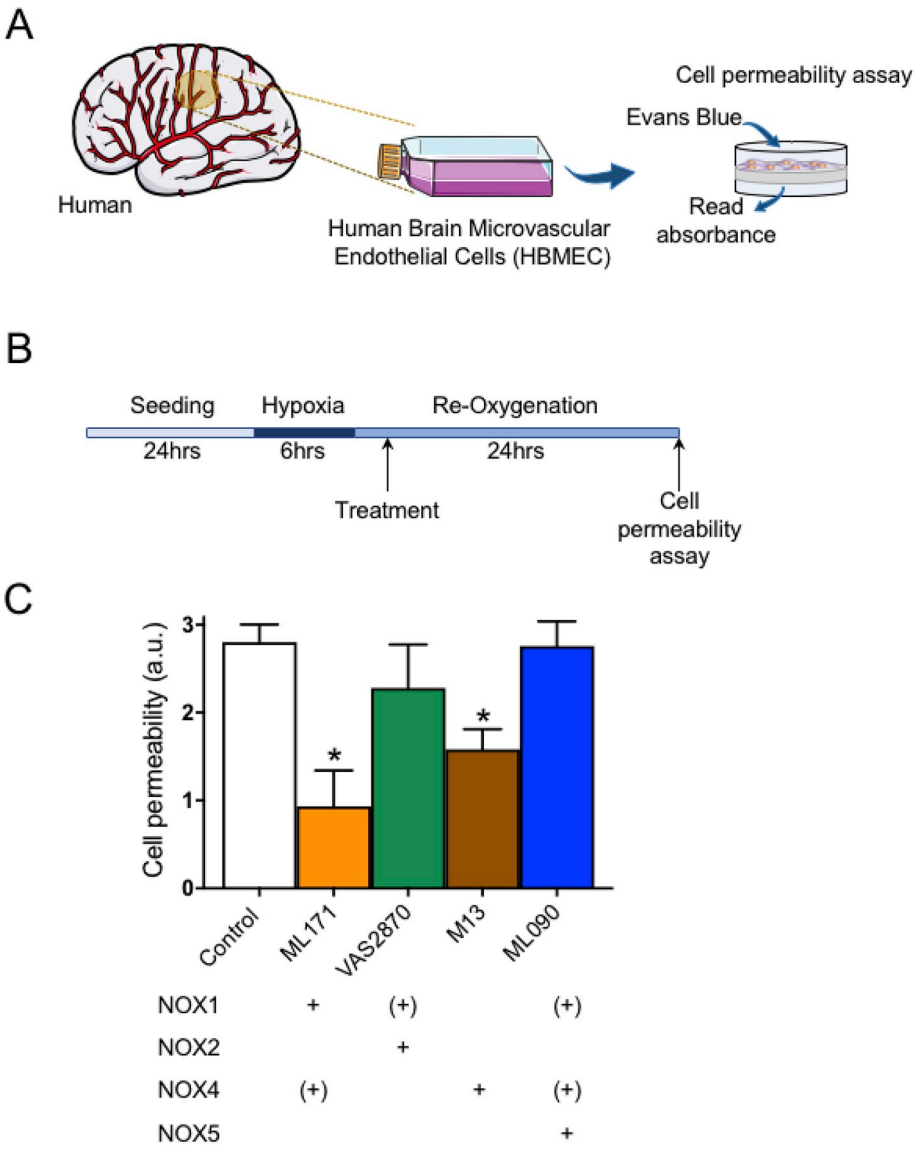

Fig. 5. ML171 and M13 inhibit ischemia-induced hyperpermeability. (A/B) HCMECs were subjected to 6hrs hypoxia followed by 24hrs re-oxygenation during which inhibitors were present. Cell permeability was subsequently assessed by measuring Evans Blue (EB) fluorescence. (C) Hypoxia caused hyperpermeability (open bar) which was significantly reduced in cells treated with ML171 (0.1 μM) or M13 (0.2 μM) while VAS2870 (0.6 μM) or ML090 (0.01 μM) treatment had no effect. Data are presented as the mean ± SEM of 4–6 experiments; *P < 0.05.

signal was enhanced (Fig. 4B).

To study non-specific antioxidant effects of VAS2870, the effect of 10 μM VAS2870 was studied in a cell-free system in presence of cytochrome C, and X/XO-derived ROS. In these assays, VAS2870 showed significant antioxidant effects (Fig. 4C).

To study whether the effects of GKT136901, ML171, VAS2870, M13 and ML090 on NOX4 and NOX5 are specific, a cell-free assay was performed with NOX4 or NOX5 effective concentrations of each inhibitor in presence of 0.25 μM H_2O_2 in an Amplex Red assay. ML171, VAS2870, M13 and ML090 did not directly affect Amplex Red-based detection of H_2O_2 (Fig. 4D). However, GKT136901 reduced Amplex Red-based H_2O_2 signals suggesting assay interference. Hence, the assay was repeated without H_2O_2 to study potential direct assay component interference. Indeed, GKT136901, ML171, M13 and ML090 reduced the signal as compared to the control (Fig. 4E) whereas in the presence of VAS2870 the signal was enhanced (Fig. 4E).

Our data suggest that none of the current NOX inhibitors could be viewed as sufficiently isoform selective, but that a panel of NOX inhibitors may be feasible for pharmacological validation of a specific NOX isoforms in a (patho)physiological process. Because of the plethora of assay artefacts and direct ROS scavenging by GKT136901, this compound was thus excluded from the panel.

3.4. Target validation of NOX in ischemia-induced hyperpermeability model

We thus tested our NOX inhibitor panel in an *in vitro* human model of ischemia-induced hyperpermeability (Fig. 5A) where NOX4 is involved in subacute hypoxia-induced increases in cell permeability [16,45], whereas NOX1, NOX2 do not [45] and NOX5 only acutely [19]. Primary HBMEC cultures were subjected to 6h of hypoxia followed by 24h of re-oxygenation (Fig. 5B) in presence or absence of NOX inhibitors using the IC_{50} concentrations to target one NOX isoform in a relatively specific manner over the other isoforms, i.e. ML171 at 0.1 μM mainly targeting NOX1; VAS203 (0.6 μM, NOX2); M13 (0.2 μM, NOX4); or ML090 (0.01 μM, NOX5). Hypoxia increased cell permeability after 24hrs of re-oxygenation. As predicted from the inhibitor screen, M13 or ML171 protected against this detrimental effect (Fig. 5C), suggesting protection against hyperpermeability via NOX4 inhibition while, as

expected given their respective IC_{50} values, VAS2870 or ML090 treatment showed no effect (Fig. 5C). These data provide a proof-of-concept for pharmacological target validation using NOX inhibitor panels.

4. Discussion

Here we present the isoform-selectivity of five widely used NOX inhibitors. Our results show that NOX-specific and isoform-selective pharmacological NOX inhibition is in principle achievable. Individual compound specificity, however, is as yet insufficient. None of the selected small molecule inhibitors were sufficiently 'isoform selective' to be used on their own. All compounds inhibited several NOX isoforms, yet with different potencies (IC_{50} values). In addition, (i) their mechanism of action and binding site is unclear, and (ii) assay interferences in addition to those that had been previously noted [46–48] needed to be taken into consideration. Nevertheless, when examining a human cell-based *in-vitro* model where NOX4 is a genetically validated causal ROS source, combining four NOX inhibitors into a panel NOX4 could be pharmacologically re-validated. Our data just provide also a proof-of-principle that similar approaches are now in principle possible for pharmacological target validation where gene KO is not an option.

With respect to the individual NOX inhibitor compounds in this study, VAS2870 has beneficial effects in several preclinical disease models such as stroke [45], Alzheimer's disease [49], thrombosis [50] and pulmonary hypertension [51]. This compound has been designated as a pan-NOX inhibitor [52] as inhibition of NOX1 [28,53], NOX2 [28,53,54], NOX4 [28,45] and NOX5 [28] has been observed. IC_{50} values for VAS2870 have been previously published for NOX2 [54,55] and recently for all the other NOX isoforms [48]. Based on the IC_{50} values reported in the present study, VAS2870 shows a slight preference for NOX2 (IC_{50} ~ 0.7 μM), over NOX1 and NOX4, which are inhibited in the lower micromolar range, and NOX5, in the higher micromolar range, in line with a recent study using two ROS assays, Amplex Red and WST-1 [48]. With respect to non-specific effects, VAS2870 slightly interfered with luminol and Amplex Red and XO-generated ROS indicating antioxidant properties as has been reported previously [24]. The latter did, however, not preclude the interpretation of NOX inhibition because the interference with XO-generated ROS was 9.6% (see Fig. 4C), inhibition of the NOX2-dependent signal, 91.5% (see Fig. 3C).

M13, a previously unreported compound from Glucox Biotech, was identified here as a first-in-class relative NOX4 selective inhibitor, 200-times more potent in inhibiting NOX4 (IC_{50} ~ 0.01 μM) versus NOX1 (IC_{50} ~ 0.2 μM), negligible NOX2 inhibition and almost no effect on NOX5. Also, M13 interfered with the Amplex Red assay by 9% (see Fig. 4E), which again did not impair the interpretation of results, as this was less than the 40% reduction of the NOX4-dependent ROS signal (see Fig. 3D). Our findings thus support further lead optimization of this promising new pharmacophore as a potentially clinically important selective NOX4 inhibitor, e.g. in stroke [45,56].

ML090 was previously described as NOX1 selective [57]. In our hands, however, its IC_{50} values for NOX1, 4 and 5 were similar suggesting that this compound is rather pan NOX inhibitor. Again two interferences were observed. ML090 lowered the Amplex Red signal 11.9% (see Fig. 4E); the NOX5 dependent ROS signal, however, was reduced by 46.8% (see Fig. 3E), suggesting a true inhibition. With respect to luminol, ML090 surprisingly increased the signal by 13.4% (see Fig. 4B); thus, the absolute 36.8% inhibition of the NOX1-dependent ROS signal (see Fig. 3D) appears to underestimate absolute efficacy for this isoform. Therapeutically, ML090 protects from vascular dysfunction in a rabbit model, an effect that has been attributed to NOX1 inhibition [58]. Based on the data presented here, however, an effect involving NOX4 and, in particular, NOX5 cannot be excluded as rabbits, unlike mice and rats, do express this isoform as well.

GKT136901, a chemical analogue and pharmacological sibling of the clinically most advanced NOX inhibitor, GKT831 (setanaxib), is widely referred to as a combined NOX1/NOX4-specific inhibitor. This compound presented, however, several problematic features and stood out amongst all compounds with respect to assay interference. GKT136901 interfered both with the Amplex Red assay for NOX4 and 5 and the luminol assay for NOX1. Moreover, it directly scavenged ROS. This latter antioxidant effect has been observed also for H_2O_2 [47,48] and peroxynitrite [30]. These characteristics thus appear to limit the interpretability of results using GKT136901 as a NOX1/NOX4 inhibitor and structurally related compounds, which is why we decided not to include this compound into our NOX inhibitor panel.

Finally, the fifth compound tested, the phenothiazine derivative, ML171, had been published as being NOX1-specific [59] with beneficial effects in models of hypertension [60], diabetes [61] and cancer [62]. We also observed a potent NOX4 and NOX5 inhibition at slightly higher concentrations, suggesting only a relative but not absolute NOX1 selectivity. Again, also this compound presented assay interferences with both Amplex Red and luminol in line with a previous observation [63]. This is most likely due to the fact that phenothiazines are peroxidase substrates [64]. The latter did, however, not preclude the interpretation of NOX1 inhibition because the assay interference was 13.4% (see Fig. 4B), whereas the NOX1-dependent signal was inhibited by 55% (see Fig. 3B).

Thus most ROS probes and the here examined NOX inhibitors are prone to artefacts (see also review in Ref. [65]). Results with NOX inhibitors on the quantification of NOX-derived ROS will need careful interpretation and require several reagent and assay controls. However, with the exception of GKT136901 this does not preclude the interpretability of functional experiments on the involvement of a given NOX isoform or not. For VAS2870, M13, ML090 and ML171 clear NOX-dependent effects were detectable in our cell-based assay.

With respect to the pharmacological validation of a specific NOX isoform, the lack of sufficient isoform selectivity of VAS2870, M13, ML090 and ML171 required to move to a NOX inhibitor panel. All compounds were used at cell-based IC_{50} concentrations and tested in a genetically pre-validated model for NOX4 to investigate whether NOX4 could be re-validated pharmacologically. In this *in-vitro* blood brain barrier model, NOX4 causes a sub-acute increase in permeability. Indeed, we observed that subacute addition of M13 (NOX4) and ML171 (NOX1 > NOX4 = NOX5) were neuroprotective, in contrast to VAS2870 (NOX2 > NOX1 > NOX5) ML090 (NOX5 > NOX 1 = NOX4 > NOX2). These panel effects suggested that NOX4 is the responsible isoform in this subacute model in accordance with previous data that established the involvement of NOX4 in the same model using genetic approaches [16,45]. The protective effect of ML171 here is attributed to inhibition of NOX4, which does, however, not exclude that inhibitory of effect of this compound in other models may be due to other isoforms such as NOX1. This, should, however, be tested using an inhibitor panel approach and not based on single compounds with limited selectivity. The inhibitor panel approach appears in principle to be feasible for pharmacological target validation of NOX in cell-based systems. Further validation in other *in-vitro* disease and models is needed.

In summary, all tested NOX inhibitor compounds displayed different apparent NOX isoform selectivity profiles suggesting differential chemical targeting of different NOX isoforms using small molecules is in principle possible. These and similar data [48] should stimulate focused library synthesis and structure-activity programs for further lead optimization to obtain eventually isoform selective small molecules for single compound target validation and potentially for clinical development. For now, we provide an immediately applicable inhibitor panel approach that allows target validation of NOXs under conditions where gene knock-out or knock-in are not feasible or, because of compensation mechanisms, not desirable.

Author contributions

H.H.H.W.S., V.T.D, S.A and M.H.E designed research; V.T.D., S.A, M.H.E, P.L, A.I.C, M.P.P, C.N and U.K performed research; V.T.D, S.A, A.I.C, M.H.E and H.H.H.W.S. analyzed and interpreted data; V.T.D and M.H.E contributed in writing and revised the final manuscript and figures; M.H.E, V.T.D. and H.H.H.W.S. wrote and edited figures and manuscript.

Declaration of competing interest

None to declare.

Acknowledgements

We wish to thank Dr. Per Wikström for providing M13, Dr. V. Jaquet for experimental advice and Dr. Merlijn J. Meens for reading the manuscript and helpful discussions. Technical assistance by P. Lijnen and J. Bost is gratefully acknowledged. Financial support (to HHHWS) by the ERC (AdG RadMed '294683' and PoC SAVEBRAIN '737586') and the Horizon 2020 programme (REPO-TRIAL '777111') is gratefully acknowledged.

Abbreviations

HBMEC	Human brain microvascular endothelial cells
HRP	Horseradish peroxidase
NOX	NADPH oxidase
PMA	Phorbol myristate acetate
ROS	Reactive oxygen species
XO	Xanthine oxidase

Appendix A. Supplementary data

Supplementary data to this article can be found online at https://doi.org/10.1016/j.freeradbiomed.2019.12.038.

References

[1] Y. Dotan, et al., No evidence supports vitamin E indiscriminate supplementation, Biofactors 35 (6) (2009) 469–473.
[2] E.R. Miller, et al., Meta-analysis: high-dosage vitamin E supplementation may increase all-cause mortality, Ann. Intern. Med. 142 (1) (2005) 37–46.
[3] G. Bjelakovic, et al., Mortality in randomized trials of antioxidant supplements for primary and secondary prevention: systematic review and meta-analysis, J. Am. Med. Assoc. 297 (8) (2007) 842–857.
[4] H.O.P.E.S. Investigators, et al., Vitamin E supplementation and cardiovascular events in high-risk patients, N. Engl. J. Med. 342 (3) (2000) 154–160.
[5] L.J. Roberts, 2nd, et al., The relationship between dose of vitamin E and suppression of oxidative stress in humans, Free Radic. Biol. Med. 43 (10) (2007) 1388–1393.
[6] K. Wingler, et al., NOX1, 2, 4, 5: counting out oxidative stress, Br. J. Pharmacol. 164 (3) (2011) 866–883.
[7] K. Bedard, K.-H. Krause, The NOX family of ROS-generating NADPH oxidases: physiology and pathophysiology, Physiol. Rev. 87 (1) (2007) 245–313.
[8] P.D. Ray, et al., Reactive oxygen species (ROS) homeostasis and redox regulation in cellular signaling, Cell. Signal. 24 (5) (2012) 981–990.
[9] T. Finkel, Signal transduction by reactive oxygen species, J. Cell Biol. 194 (1) (2011) 7–15.
[10] V.T. Dao, et al., Pharmacology and clinical drug candidates in redox medicine, Antioxidants Redox Signal. 23 (14) (2015) 1113–1129.
[11] M.H. Elbatreek, et al., Reactive oxygen comes of age: mechanism-based therapy of diabetic end-organ damage, Trends Endocrinol. Metab.: TEM (Trends Endocrinol. Metab.) 30 (5) (2019) 312–327.
[12] A.I. Casas, et al., Reactive oxygen-related diseases: therapeutic targets and emerging clinical indications, Antioxidants Redox Signal. 23 (14) (2015) 1171–1185.
[13] S.P. Gray, et al., NADPH oxidase 1 plays a key role in diabetes mellitus-accelerated atherosclerosis, Circulation 127 (18) (2013) 1888–1902.
[14] J.L. Wilkinson-Berka, et al., NADPH oxidase, NOX1, mediates vascular injury in ischemic retinopathy, Antioxidants Redox Signal. (2013).
[15] S. Sorce, K.H. Krause, NOX enzymes in the central nervous system: from signaling to disease, Antioxidants Redox Signal. 11 (10) (2009) 2481–2504.
[16] A.I. Casas, et al., NOX4-dependent neuronal autotoxicity and BBB breakdown explain the superior sensitivity of the brain to ischemic damage, Proc. Natl. Acad. Sci. U.S.A. 114 (46) (2017) 12315–12320.
[17] J.C. Jha, et al., Genetic targeting or pharmacologic inhibition of NADPH oxidase Nox4 provides renoprotection in long-term diabetic nephropathy, J. Am. Soc. Nephrol. : JASN (J. Am. Soc. Nephrol.) (2014).
[18] C. Geis, et al., NOX4 is an early initiator of neuropathic pain, Exp. Neurol. 288 (2017) 94–103.
[19] A.I. Casas, et al., Calcium-dependent blood-brain barrier breakdown by NOX5 limits postreperfusion benefit in stroke, J. Clin. Investig. 130 (4) (2019) 1772–1778.
[20] C.E. Holterman, et al., Nephropathy and elevated BP in mice with podocyte-specific NADPH oxidase 5 expression, J. Am. Soc. Nephrol. : JASN (2013) ASN.2013040371.
[21] J.C. Jha, et al., NADPH oxidase Nox5 accelerates renal injury in diabetic nephropathy, Diabetes 66 (10) (2017) 2691–2703.
[22] D. Pandey, et al., Expression and functional significance of NADPH oxidase 5 (Nox5) and its splice variants in human blood vessels, Am. J. Physiol. Heart Circ. Physiol. 302 (10) (2012) H1919–H1928.
[23] T.J. Guzik, et al., Calcium-dependent NOX5 nicotinamide adenine dinucleotide phosphate oxidase contributes to vascular oxidative stress in human coronary artery disease, J. Am. Coll. Cardiol. 52 (22) (2008) 1803–1809.
[24] S. Altenhöfer, et al., Evolution of NADPH oxidase inhibitors: selectivity and mechanisms for target engagement, Antioxidants Redox Signal. 23 (5) (2015) 406–427.
[25] S.P. Gray, et al., NADPH oxidase 1 plays a key role in diabetes mellitus-accelerated atherosclerosis, Circulation 127 (18) (2013) 1888–1902.
[26] S.P. Gray, et al., Reactive oxygen species can provide atheroprotection via NOX4-dependent inhibition of inflammation and vascular remodeling, Arterioscler. Thromb. Vasc. Biol. 36 (2) (2016) 295–307.
[27] C. Schürmann, et al., The NADPH oxidase Nox4 has anti-atherosclerotic functions, Eur. Heart J. 36 (48) (2015) 3447–3456.
[28] S. Altenhöfer, et al., The NOX toolbox: validating the role of NADPH oxidases in physiology and disease, Cell. Mol. Life Sci. 69 (14) (2012) 2327–2343.
[29] S. Heumüller, et al., Apocynin is not an inhibitor of vascular NADPH oxidases but an antioxidant, Hypertension 51 (2) (2008) 211–217.
[30] S. Schildknecht, et al., The NOX1/4 inhibitor GKT136901 as selective and direct scavenger of peroxynitrite, Curr. Med. Chem. 21 (3) (2014) 365–376.
[31] J. Zielonka, et al., High-throughput assays for superoxide and hydrogen peroxide: design of a screening workflow to identify inhibitors of NADPH oxidases, J. Biol. Chem. 289 (23) (2014) 16176–16189.
[32] J. Zielonka, et al., On the use of L-012, a luminol-based chemiluminescent probe, for detecting superoxide and identifying inhibitors of NADPH oxidase: a reevaluation, Free Radical Biol. Med. 65 (2013) 1310–1314.
[33] S. Wind, et al., Comparative pharmacology of chemically distinct NADPH oxidase inhibitors, Br. J. Pharmacol. 161 (4) (2010) 885–898.
[34] O. Teufelhofer, et al., Promyelocytic HL60 cells express NADPH oxidase and are excellent targets in a rapid spectrophotometric microplate assay for extracellular superoxide, Toxicol. Sci. 76 (2) (2003) 376–383.
[35] K. Hirano, et al., Discovery of GSK2795039, a novel small molecule NADPH oxidase 2 inhibitor, Antioxidants Redox Signal. 23 (5) (2015) 358–374.
[36] G.J. Maghzal, et al., Detection of reactive oxygen species derived from the family of NOX NADPH oxidases, Free Radical Biol. Med. 53 (10) (2012) 1903–1918.
[37] D. Gianni, et al., A novel and specific NADPH oxidase-1 (Nox1) small-molecule inhibitor blocks the formation of functional invadopodia in human colon cancer cells, ACS Chem. Biol. 5 (10) (2010) 981–993.
[38] D. Gianni, et al., Optimization and characterization of an inhibitor for NADPH oxidase 1 (NOX-1), Probe Reports from the NIH Molecular Libraries Program, 2010.
[39] S. Wind, et al., Comparative pharmacology of chemically distinct NADPH oxidase inhibitors, Br. J. Pharmacol. 161 (4) (2010) 885–898.
[40] X. Wang, et al., The novel NADPH oxidase 4 selective inhibitor GLX7013114 counteracts human islet cell death in vitro, PLoS One 13 (9) (2018) e0204271.
[41] Y. Nisimoto, et al., Nox4: a hydrogen peroxide-generating oxygen sensor, Biochemistry 53 (31) (2014) 5111–5120.
[42] L. Serrander, et al., NOX4 activity is determined by mRNA levels and reveals a unique pattern of ROS generation, Biochem. J. 406 (1) (2007) 105–114.
[43] L. Serrander, et al., NOX5 is expressed at the plasma membrane and generates superoxide in response to protein kinase C activation, Biochimie 89 (9) (2007) 1159–1167.
[44] F. Chen, et al., Nox5 stability and superoxide production is regulated by C-terminal binding of Hsp90 and CO-chaperones, Free Radic. Biol. Med. 89 (2015) 793–805.
[45] C. Kleinschnitz, et al., Post-stroke inhibition of induced NADPH oxidase type 4 prevents oxidative stress and neurodegeneration, PLoS Biol. 8 (9) (2010).
[46] S. Altenhofer, et al., Evolution of NADPH oxidase inhibitors: selectivity and mechanisms for target engagement, Antioxidants Redox Signal. 23 (5) (2015) 406–427.
[47] K.D. Martyn, et al., Functional analysis of Nox4 reveals unique characteristics compared to other NADPH oxidases, Cell. Signal. 18 (1) (2006) 69–82.
[48] F. Augsburger, et al., Pharmacological characterization of the seven human NOX isoforms and their inhibitors, Redox Biol. 26 (2019) 101272.
[49] A.A. Abubaker, et al., Amyloid peptide beta1-42 induces integrin alphaIIbbeta3 activation, platelet adhesion, and thrombus formation in a NADPH oxidase-dependent manner, Oxid. Med. Cell Longev. 2019 (2019) 1050476.
[50] P.V. Avdonin, et al., VAS2870 inhibits histamine-induced calcium signaling and vWF secretion in human umbilical vein endothelial cells, Cells 8 (2) (2019).
[51] T. Li, et al., Magnesium lithospermate B prevents phenotypic transformation of pulmonary arteries in rats with hypoxic pulmonary hypertension through suppression of NADPH oxidase, Eur. J. Pharmacol. 847 (2019) 32–41.
[52] K. Wingler, et al., VAS2870 is a pan-NADPH oxidase inhibitor, Cell. Mol. Life Sci. 69 (18) (2012) 3159–3160.

[53] S. Wind, et al., Oxidative stress and endothelial dysfunction in aortas of aged spontaneously hypertensive rats by NOX1/2 is reversed by NADPH oxidase inhibition, Hypertension 56 (3) (2010) 490–497.
[54] G.J. Gatto, et al., NADPH oxidase-dependent and -independent mechanisms of reported inhibitors of reactive oxygen generation, J. Enzym. Inhib. Med. Chem. 28 (1) (2013) 95–104.
[55] H. ten Freyhaus, et al., Novel Nox inhibitor VAS2870 attenuates PDGF-dependent smooth muscle cell chemotaxis, but not proliferation, Cardiovasc. Res. 71 (2) (2006) 331–341.
[56] A.I. Casas, et al., NOX4-dependent neuronal autotoxicity and BBB breakdown explain the superior sensitivity of the brain to ischemic damage, Proc. Natl. Acad. Sci. U. S. A. (2017).
[57] S.J. Brown, et al., Probe Report for NOX1 Inhibitors, (2010).
[58] R.M. Smith, et al., Role of Nox inhibitors plumbagin, ML090 and gp91ds-tat peptide on homocysteine thiolactone induced blood vessel dysfunction, Clin. Exp. Pharmacol. Physiol. 42 (8) (2015) 860–864.
[59] D. Gianni, et al., A novel and specific NADPH oxidase-1 (Nox1) small-molecule inhibitor blocks the formation of functional invadopodia in human colon cancer cells, ACS Chem. Biol. 5 (10) (2010) 981–993.
[60] A.P. Harvey, et al., Vascular dysfunction and fibrosis in stroke-prone spontaneously hypertensive rats: the aldosterone-mineralocorticoid receptor-Nox1 axis, Life Sci. 179 (2017) 110–119.
[61] J.R. Weaver, et al., Inhibition of NADPH oxidase-1 preserves beta cell function, Diabetologia 58 (1) (2015) 113–121.
[62] S. Liang, et al., NADPH oxidase 1 in liver macrophages promotes inflammation and tumor development in mice, Gastroenterology 156 (4) (2019) 1156–1172 e6.
[63] T. Seredenina, et al., A subset of N-substituted phenothiazines inhibits NADPH oxidases, Free Radical Biol. Med. 86 (2015) 239–249.
[64] T.V. Rogozhina, V.V. Rogozhin, [Phenothiazines are slowly oxidizable substrates of horseradish peroxidase], Biomeditsinskaia khimiia 57 (5) (2011) 544–553.
[65] G.J. Maghzal, et al., Detection of reactive oxygen species derived from the family of NOX NADPH oxidases, Free Radic. Biol. Med. 53 (10) (2012) 1903–1918.